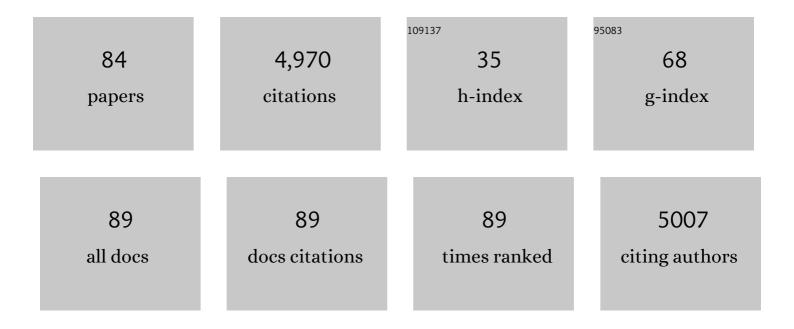
List of Publications by Year in descending order

Source: https://exaly.com/author-pdf/7744069/publications.pdf Version: 2024-02-01



HAO ZHENC

#	Article	IF	CITATIONS
1	Impacts of adding biochar on nitrogen retention and bioavailability in agricultural soil. Geoderma, 2013, 206, 32-39.	2.3	365
2	Investigating the mechanisms of biochar's removal of lead from solution. Bioresource Technology, 2015, 177, 308-317.	4.8	337
3	Sorption of antibiotic sulfamethoxazole varies with biochars produced at different temperatures. Environmental Pollution, 2013, 181, 60-67.	3.7	334
4	Characteristics and nutrient values of biochars produced from giant reed at different temperatures. Bioresource Technology, 2013, 130, 463-471.	4.8	301
5	Use of biochar-compost to improve properties and productivity of the degraded coastal soil in the Yellow River Delta, China. Journal of Soils and Sediments, 2017, 17, 780-789.	1.5	208
6	Enhanced growth of halophyte plants in biocharâ€amended coastal soil: roles of nutrient availability and rhizosphere microbial modulation. Plant, Cell and Environment, 2018, 41, 517-532.	2.8	194
7	Photodegradation Elevated the Toxicity of Polystyrene Microplastics to Grouper (<i>Epinephelus) Tj ETQq1 1 0. 2020, 54, 6202-6212.</i>	784314 rgl 4.6	BT /Overloc 187
8	Formation and Physicochemical Characteristics of Nano Biochar: Insight into Chemical and Colloidal Stability. Environmental Science & Technology, 2018, 52, 10369-10379.	4.6	178
9	Biochar-induced negative carbon mineralization priming effects in a coastal wetland soil: Roles of soil aggregation and microbial modulation. Science of the Total Environment, 2018, 610-611, 951-960.	3.9	170
10	Characterization and influence of biochars on nitrous oxide emission from agricultural soil. Environmental Pollution, 2013, 174, 289-296.	3.7	156
11	Combined effects of biochar properties and soil conditions on plant growth: A meta-analysis. Science of the Total Environment, 2020, 713, 136635.	3.9	156
12	Lithium Difluorophosphateâ€Based Dualâ€Salt Low Concentration Electrolytes for Lithium Metal Batteries. Advanced Energy Materials, 2020, 10, 2001440.	10.2	121
13	Reduced nitrification and abundance of ammonia-oxidizing bacteria in acidic soil amended with biochar. Chemosphere, 2015, 138, 576-583.	4.2	107
14	Comparative toxicity of the plasticizer dibutyl phthalate to two freshwater algae. Aquatic Toxicology, 2017, 191, 122-130.	1.9	87
15	Biodegradable and re-usable sponge materials made from chitin for efficient removal of microplastics. Journal of Hazardous Materials, 2021, 420, 126599.	6.5	77
16	In-Situ Ligand Formation-Driven Preparation of a Heterometallic Metal–Organic Framework for Highly Selective Separation of Light Hydrocarbons and Efficient Mercury Adsorption. ACS Applied Materials & Interfaces, 2016, 8, 23331-23337.	4.0	72
17	Production and characterization of hydrochars and their application in soil improvement and environmental remediation. Chemical Engineering Journal, 2022, 430, 133142.	6.6	71
18	Sequential combination of photocatalysis and microalgae technology for promoting the degradation and detoxification of typical antibiotics. Water Research, 2022, 210, 117985.	5.3	70

#	Article	IF	CITATIONS
19	Environmental life cycle assessment of wheat production using chemical fertilizer, manure compost, and biochar-amended manure compost strategies. Science of the Total Environment, 2021, 760, 143342.	3.9	69
20	Comparative study of individual and Co-Application of biochar and wood vinegar on blueberry fruit yield and nutritional quality. Chemosphere, 2020, 246, 125699.	4.2	66
21	Biochar addition reduced net N mineralization of a coastal wetland soil in the Yellow River Delta, China. Geoderma, 2016, 282, 120-128.	2.3	65
22	Coadsorption, desorption hysteresis and sorption thermodynamics of sulfamethoxazole and carbamazepine on graphene oxide and graphite. Carbon, 2013, 65, 243-251.	5.4	64
23	Aging impacts of low molecular weight organic acids (LMWOAs) on furfural production residue-derived biochars: Porosity, functional properties, and inorganic minerals. Science of the Total Environment, 2017, 607-608, 1428-1436.	3.9	64
24	Characteristics and mechanisms of chlorpyrifos and chlorpyrifos-methyl adsorption onto biochars: Influence of deashing and low molecular weight organic acid (LMWOA) aging and co-existence. Science of the Total Environment, 2019, 657, 953-962.	3.9	62
25	TMED3 promotes hepatocellular carcinoma progression via IL-11/STAT3 signaling. Scientific Reports, 2016, 6, 37070.	1.6	61
26	Differential toxicity of functionalized polystyrene microplastics to clams (Meretrix meretrix) at three key development stages of life history. Marine Pollution Bulletin, 2019, 139, 346-354.	2.3	54
27	Effects of biochar on carbon mineralization of coastal wetland soils in the Yellow River Delta, China. Ecological Engineering, 2016, 94, 329-336.	1.6	53
28	Polystyrene microplastics impaired the feeding and swimming behavior of mysid shrimp Neomysis japonica. Marine Pollution Bulletin, 2020, 150, 110660.	2.3	49
29	Pyrolysis of Arundo donax L. to produce pyrolytic vinegar and its effect on the growth of dinoflagellate Karenia brevis. Bioresource Technology, 2018, 247, 273-281.	4.8	44
30	Effect of co-application of wood vinegar and biochar on seed germination and seedling growth. Journal of Soils and Sediments, 2019, 19, 3934-3944.	1.5	44
31	Efficacies of biochar and biochar-based amendment on vegetable yield and nitrogen utilization in four consecutive planting seasons. Science of the Total Environment, 2017, 593-594, 124-133.	3.9	43
32	Biochar decreased enantioselective uptake of chiral pesticide metalaxyl by lettuce and shifted bacterial community in agricultural soil. Journal of Hazardous Materials, 2021, 417, 126047.	6.5	43
33	CBX6 overexpression contributes to tumor progression and is predictive of a poor prognosis in hepatocellular carcinoma. Oncotarget, 2017, 8, 18872-18884.	0.8	42
34	Biochar reduced Chinese chive (Allium tuberosum) uptake and dissipation of thiamethoxam in an agricultural soil. Journal of Hazardous Materials, 2020, 390, 121749.	6.5	41
35	MicroRNA‑197‑3p acts as a prognostic marker and inhibits cell invasion in hepatocellular carcinoma. Oncology Letters, 2019, 17, 2317-2327.	0.8	38
36	Characteristics of algae-derived biochars and their sorption and remediation performance for sulfamethoxazole in marine environment. Chemical Engineering Journal, 2022, 430, 133092.	6.6	38

#	Article	IF	CITATIONS
37	Individual and combined applications of biochar and pyroligneous acid mitigate dissemination of antibiotic resistance genes in agricultural soil. Science of the Total Environment, 2021, 796, 148962.	3.9	37
38	miR-515–5p suppresses HCC migration and invasion via targeting IL6/JAK/STAT3 pathway. Surgical Oncology, 2020, 34, 113-120.	0.8	36
39	Adsorption, desorption and coadsorption behaviors of sulfamerazine, Pb(II) and benzoic acid on carbon nanotubes and nano-silica. Science of the Total Environment, 2020, 738, 139685.	3.9	35
40	miR-365a-3p regulates ADAM10-JAK-STAT signaling to suppress the growth and metastasis of colorectal cancer cells. Journal of Cancer, 2020, 11, 3634-3644.	1.2	33
41	Epigenetically silenced long noncoding-SRHC promotes proliferation of hepatocellular carcinoma. Journal of Cancer Research and Clinical Oncology, 2015, 141, 1195-1203.	1.2	31
42	Co-adsorption of perfluorooctane sulfonate and phosphate on boehmite: Influence of temperature, phosphate initial concentration and pH. Ecotoxicology and Environmental Safety, 2017, 137, 71-77.	2.9	31
43	Four calcium(<scp>ii</scp>) coordination polymers based on 2,5-dibromoterephthalic acid and different N-donor organic species: syntheses, structures, topologies, and luminescence properties. CrystEngComm, 2016, 18, 8664-8671.	1.3	30
44	Comparison of efficacies of peanut shell biochar and biochar-based compost on two leafy vegetable productivity in an infertile land. Chemosphere, 2019, 224, 151-161.	4.2	30
45	Pyroligneous acid mitigated dissemination of antibiotic resistance genes in soil. Environment International, 2020, 145, 106158.	4.8	29
46	Effects of biochar input on the properties of soil nanoparticles and dispersion/sedimentation of natural mineral nanoparticles in aqueous phase. Science of the Total Environment, 2018, 634, 595-605.	3.9	28
47	Tropomodulin 3 modulates ECFRâ€PI3Kâ€AKT signaling to drive hepatocellular carcinoma metastasis. Molecular Carcinogenesis, 2019, 58, 1897-1907.	1.3	27
48	Phase behavior of ovalbumin and carboxymethylcellulose composite system. Carbohydrate Polymers, 2014, 109, 64-70.	5.1	25
49	Functionalized polystyrene nanoplastic-induced energy homeostasis imbalance and the immunomodulation dysfunction of marine clams (<i>Meretrix meretrix</i>) at environmentally relevant concentrations. Environmental Science: Nano, 2021, 8, 2030-2048.	2.2	25
50	Stable sodium metal anode enhanced by advanced electrolytes with SbF3 additive. Rare Metals, 2021, 40, 433-439.	3.6	24
51	elF5B increases ASAP1 expression to promote HCC proliferation and invasion. Oncotarget, 2016, 7, 62327-62339.	0.8	24
52	Inhibitory mechanism of phthalate esters on Karenia brevis. Chemosphere, 2016, 155, 498-508.	4.2	23
53	Fate of four phthalate esters with presence of Karenia brevis: Uptake and biodegradation. Aquatic Toxicology, 2019, 206, 81-90.	1.9	23
54	Flood Risk Assessment Based on Fuzzy Synthetic Evaluation Method in the Beijing-Tianjin-Hebei Metropolitan Area, China. Sustainability, 2020, 12, 1451.	1.6	23

HAO ZHENG

#	Article	IF	CITATIONS
55	Comparative study of pyrochar and hydrochar on peanut seedling growth in a coastal salt-affected soil of Yellow River Delta, China. Science of the Total Environment, 2022, 833, 155183.	3.9	23
56	M ⁶ A-mediated up-regulation of LncRNA LIFR-AS1 enhances the progression of pancreatic cancer via miRNA-150-5p/ VEGFA/Akt signaling. Cell Cycle, 2021, 20, 2507-2518.	1.3	22
57	Removal of micro organic pollutants in high salinity wastewater by comproportionation system of Fe(VI)/Fe(III): Enhancement of chloride and bicarbonate. Water Research, 2022, 214, 118182.	5.3	22
58	Comparison of different crop residue-based technologies for their energy production and air pollutant emission. Science of the Total Environment, 2020, 707, 136122.	3.9	21
59	Direct Spectroscopic Evidence for Charge-Assisted Hydrogen-Bond Formation between Ionizable Organic Chemicals and Carbonaceous Materials. Environmental Science & Technology, 2022, 56, 9356-9366.	4.6	19
60	Effect of Biochar on the Enantioselective Soil Dissipation and Lettuce Uptake and Translocation of the Chiral Pesticide Metalaxyl in Contaminated Soil. Journal of Agricultural and Food Chemistry, 2019, 67, 13550-13557.	2.4	17
61	Decreased Expression of Programmed Death Ligand-L1 by Seven in Absentia Homolog 2 in Cholangiocarcinoma Enhances T-Cell–Mediated Antitumor Activity. Frontiers in Immunology, 2022, 13, 845193.	2.2	16
62	Heparin and rosuvastatin calcium-loaded poly(<scp>l</scp> -lactide-co-caprolactone) nanofiber-covered stent-grafts for aneurysm treatment. New Journal of Chemistry, 2017, 41, 9014-9023.	1.4	15
63	Constructed wetlands for rural domestic wastewater treatment: A coupling of tidal strategy, in-situ bio-regeneration of zeolite and Fe(â;)-oxygen denitrification. Bioresource Technology, 2022, 344, 126185.	4.8	15
64	Modified Cellulose Nanocrystals Enhanced the Compatibility Between PLA and PBAT to Prepare a Multifunctional Composite Film. Journal of Polymers and the Environment, 2022, 30, 3139-3149.	2.4	14
65	Biochar for Water and Soil Remediation: Production, Characterization, and Application. , 2020, , 153-196.		13
66	MiR-499a-5p promotes 5-FU resistance and the cell proliferation and migration through activating PI3K/Akt signaling by targeting PTEN in pancreatic cancer. Annals of Translational Medicine, 2021, 9, 1798-1798.	0.7	12
67	Low CDX1 expression predicts a poor prognosis for hepatocellular carcinoma patients after hepatectomy. Surgical Oncology, 2016, 25, 171-177.	0.8	10
68	Temporary Ischemia Time Before Snap Freezing Is Important for Maintaining High-Integrity RNA in Hepatocellular Carcinoma Tissues. Biopreservation and Biobanking, 2019, 17, 425-432.	0.5	7
69	Biochar Enhanced Growth and Biological Nitrogen Fixation of Wild Soybean (Clycine max subsp. soja) Tj ETQq1	1 0,78431 1.4	l4 rgBT /Over
70	Influences of polyethylene glycol (PEG) on the performance of LiMn2O4 cathode material for lithium ion battery. Journal of Materials Science: Materials in Electronics, 2016, 27, 5408-5414.	1.1	6
71	Water sources of riparian plants during a rainy season in Taihu Lake Basin, China: a stable isotope study. Chemical Speciation and Bioavailability, 2017, 29, 153-160.	2.0	6
72	In situ prepared algae-supported iron sulfide to remove hexavalent chromium. Environmental Pollution, 2021, 274, 115831.	3.7	6

#	Article	IF	CITATIONS
73	Modification of STIM2 by m6A RNA methylation inhibits metastasis of cholangiocarcinoma. Annals of Translational Medicine, 2022, 10, 40-40.	0.7	6
74	Spatial Patterns of Microplastics in Surface Seawater, Sediment, and Sand Along Qingdao Coastal Environment. Frontiers in Marine Science, 2022, 9, .	1.2	6
75	A SupraGel for efficient production of cell spheroids. Science China Materials, 2022, 65, 1655-1661.	3.5	4
76	TOP2 gene disruption reduces drug susceptibility by increasing intracellular ergosterol biosynthesis in Candida albicans. Journal of Medical Microbiology, 2010, 59, 797-803.	0.7	3
77	Lamp2 inhibits epithelial-mesenchymal transition by suppressing Snail expression in HCC. Oncotarget, 2018, 9, 30240-30252.	0.8	3
78	Circular RNA circ_0008934 promotes hepatocellular carcinoma growth and metastasis through modulating miR-1305/TMTC3 axis. Human Cell, 2022, 35, 498-510.	1.2	3
79	Laparoscopic transcystic common bile duct exploration in patients with a nondilated common bile duct. Annals of Palliative Medicine, 2021, 10, 12845-12856.	0.5	3
80	MicroRNA-506-3p targets SIRT1 and suppresses AMPK pathway activation to promote hepatic steatosis. Experimental and Therapeutic Medicine, 2021, 22, 1430.	0.8	2
81	Analysis of Material Properties with Biochar Improve Indian Mustard (<i>Brassica) Tj ETQq1 1 0.784314 rgBT 239-242.</i>	/Overlock 0.2	10 Tf 50 4 1
82	Solvent-mediated preparation of a heterometallic [2 × 2] grid via a 1D metal–organic template with extraordinary acid/base-resistance. RSC Advances, 2017, 7, 5578-5582.	1.7	1
83	Soft coral-derived Aspernolide A suppressed non-small cell lung cancer induced osteolytic bone invasion via the c-Fos/NFATC1 signaling pathway. Journal of Thoracic Disease, 2021, 13, 5996-6011.	0.6	1
84	[Corrigendum] MicroRNA‑506‑3p targets SIRT1 and suppresses AMPK pathway activation to promote hepatic steatosis. Experimental and Therapeutic Medicine, 2022, 24, .	0.8	0